



Microstructure development and thixoextrusion of magnesium alloy prepared by repetitive upsetting-extrusion

Qiang Chen*, Zude Zhao, Zhixiang Zhao, Chuankai Hu, Dayu Shu

Southwest Technique and Engineering Institute, Yuzhou Road 33, Chongqing 400039, PR China

ARTICLE INFO

Article history:

Received 9 October 2010

Received in revised form 21 April 2011

Accepted 21 April 2011

Available online 28 April 2011

Key words:

AZ80 magnesium alloy

Microstructure

Mechanical properties

Semi-solid

ABSTRACT

Thixoextrusion involves processing alloys with a spheroidal microstructure in the semi-solid state. Before thixoextrusion, repetitive upsetting-extrusion (RUE) is introduced into the strain induced metal activation (SIMA) process to predeform AZ80 magnesium alloy. Microstructure evolution of RUE formed AZ80 magnesium alloy during partial remelting is studied at temperatures for times. Tensile mechanical properties of thixoextruded components are determined and compared with those of AZ80 magnesium alloy thixoextruded from starting material produced by casting. The results show that with increasing number of RUE passes solid grain size decreases and the rate of liquation is improved. Prolonged holding time results in grain coarsening and the improvement of degree of spheroidization. The variation of the solid grains with holding time obeys the Lifshitz, Slyozov and Wagner law. Increasing the heating temperature is favorable for the formation of spheroidal solid grains. The tensile properties for AZ80 magnesium alloy thixoextruded from starting material produced by RUE are better than those of AZ80 magnesium alloy thixoextruded from starting material produced by casting.

© 2011 Elsevier B.V. All rights reserved.

1. Introduction

In recent years, magnesium alloys have been received special attention in the automobile industry due to their high specific strength, superior damping capacity, high thermal conductivity and good machinability [1,2]. Although high pressure die casting (HPDC) is the dominant method in manufacturing components of magnesium alloys, semi-solid processing offers significant advantages over HPDC because of near-net shape processing, better mechanical properties, less energy consumption and longer die life [3].

Thixoextrusion, which belongs to semi-solid processing, describes the process where suitable material is heated into the semi-solid state and then is hold into the die for processing [4]. Subsequently, the material in the semi-solid state is extruded to form components. For thixoextrusion to be possible, the microstructure of the starting material must be non-dendritic. It will then behave thixotropically: when the material is sheared it flows but when it is allowed to stand it thickens again; the viscosity is time and shear rate dependent [5–7]. Flow in the die is then laminar, avoiding many of the defects associated with conventional die casting. The main disadvantage of the process is that the starting material must be treated in such a way that the microstructure is spheroidal

rather than dendritic [8]. The required spheroidal microstructure can be obtained by a number of routes, including magnetohydrodynamic, sprayforming, near-liquidus casting, new MIT process, grain refinement and strain induced melt activation (SIMA). These are summarised by Atkinson [9]. The last involves hot working above recrystallisation temperature followed by some cold work prior to reheating.

Repetitive upsetting-extrusion (RUE) developed by Aizawa and Tokumitsu is a promising technique to induce a great strain in bulk metals [10]. The principle of the RUE process is shown in Fig. 1. In RUE, a sample is contained within a chamber and then the sample is upsetted and extruded repeatedly [11]. The accumulated equivalent strain is approximately given by

$$\varepsilon = 2n \ln \left(\frac{D}{d} \right) \quad (1)$$

where D is the chamber diameter, d is the channel diameter and n is the number of deformation cycles. Although some researchers introduced equal channel angular extrusion (ECAE) into SIMA [12–14], there have been no published reports about the microstructure evolution of magnesium alloys treated by RUE during partial remelting.

The present article aims to employ RUE to predeform an as-cast AZ80 magnesium alloy before partial remelting. The microstructural evolution of AZ80 magnesium alloy treated by RUE is studied. Moreover, this paper presents recent new results on mechanical

* Corresponding author.

E-mail address: 2009chenqiang@163.com (Q. Chen).

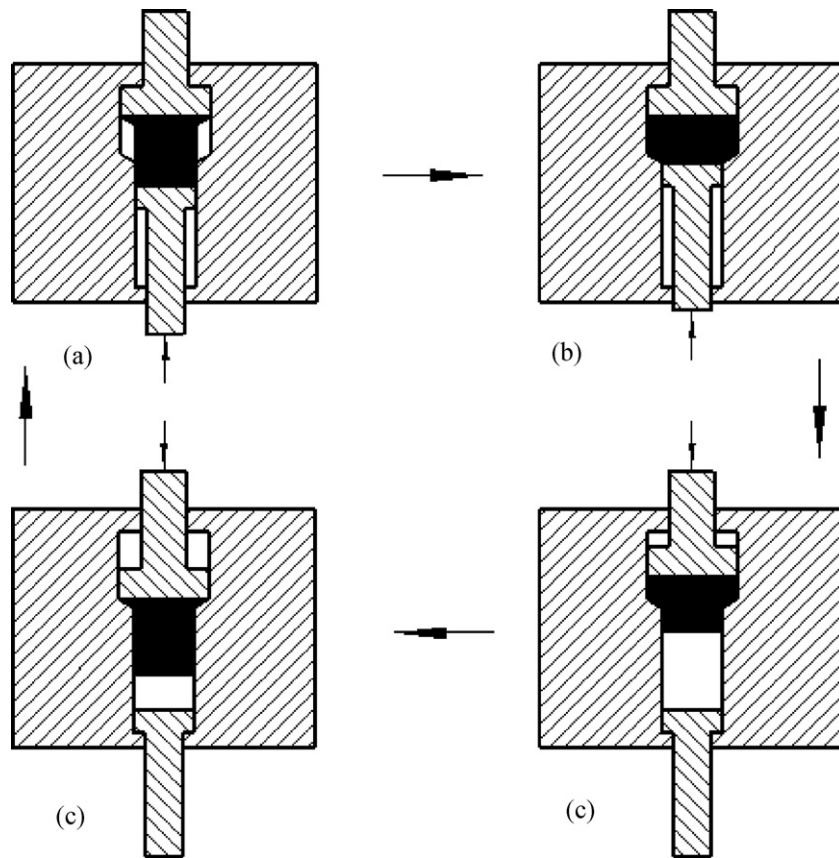


Fig. 1. Schematic illustration of repetitive upsetting-extrusion (RUE) process: (a) upsetting, (b) finish of upsetting, (c) extrusion, and (d) finish of extrusion.

properties of thixoextruded AZ80 magnesium alloy prepared by SIMA.

2. Experimental

The composition of as-cast AZ80 magnesium alloy was Mg–8.2 wt.%Al–0.45 wt.%Zn–0.21 wt.%Mn–0.18 wt.%Si, which was provided by Yin Guang Magnesium Industry Co. Ltd. The as-cast AZ80 magnesium alloy bar with a diameter of 110 mm was prepared using semi-continuous casting. The solidus and the liquidus temperatures for the as-cast AZ80 magnesium alloy were obtained as 512 °C and 613 °C from a differential scanning calorimetry (DSC) experiment at 6 °C min^{−1}. Theoretical solid fractions were calculated according to the Scheil

equation [15]:

$$f_s = 1 - \left(\frac{T_m - T}{T_m - T_L} \right)^{1/k_0 - 1} \quad (2)$$

where T_m is the melting temperature of pure metal, T_L is the liquidus temperature of the alloy and k_0 is the equilibrium distribution coefficient. In the present research, T_m and k_0 are taken as 650 °C and 0.36, respectively. The different tem-

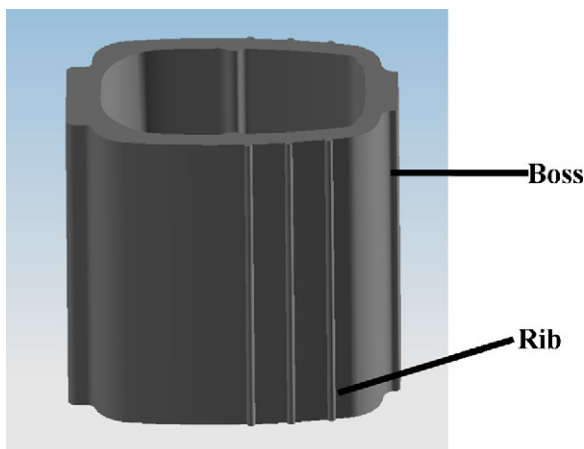


Fig. 2. The three-dimensional model of barrel-shaped component.

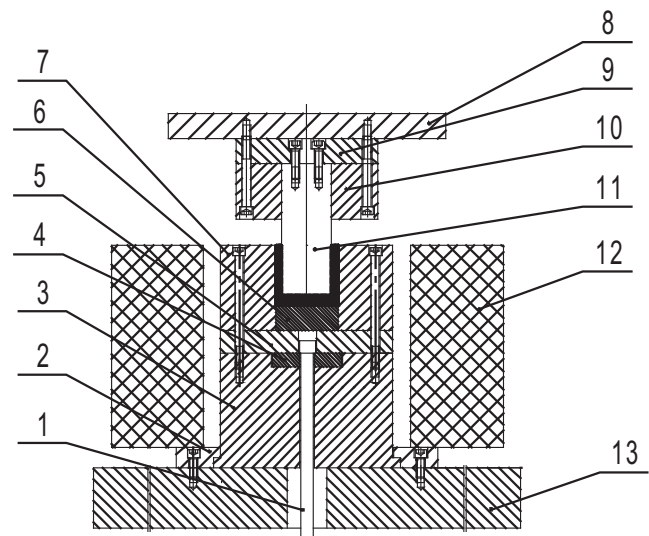


Fig. 3. 1: Carrier rod, 2: pressing ring of cavity die, 3: die shoe, 4: backing board, 5: backing board, 6: cavity die bed, 7: cavity die, 8: upper follow board, 9: backing board of male die, 10: sleeve of male die, 11: male die, 12: heating-furnace, and 13: lower backing board.

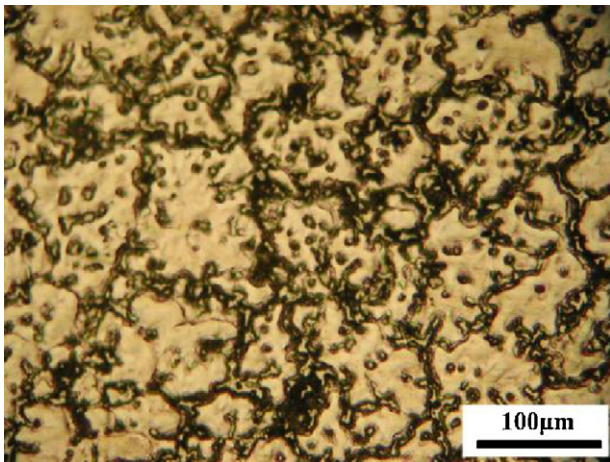


Fig. 4. Microstructure of as-cast AZ80 magnesium alloy.

peratures of 540 °C, 550 °C, 560 °C, 570 °C and 580 °C during partial remelting were predetermined in the present research. According to the Scheil equation, the corresponding theoretical solid fractions were calculated as 0.82, 0.79, 0.75, 0.70 and 0.63. Moreover, practical solid fractions were determined by image analysis software.

The as-cast AZ80 magnesium alloy bar was machined into 100 mm diameter \times 140 mm height cylinder samples for RUE. Because the diameters of the upsetting and extrusion rams were 80 mm and 100 mm, respectively, the true strain in the axial direction of the solid cylinder sample for a single upsetting or extrusion operation was 0.4463. Before RUE, the as-cast AZ80 samples were preheated at 300 °C for 80 min. At the same time, the RUE die was preheated to 300 °C. Both the samples and the die were lubricated with molybdenum disulphide (MoS_2). After deformation, samples treated by RUE were immediately quenched in cold water. In

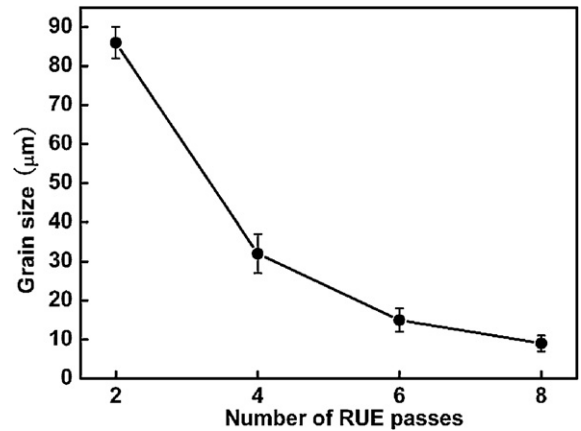


Fig. 6. Plot of grain size as a function of number of RUE passes.

the present study, the as-cast AZ80 billet was firstly objected to upsetting and then to extrusion. Therefore, after two-pass, four-pass, six-pass and eight-pass RUE, the final deformation of the billet was extrusion. During extrusion, the equivalent strain located in the edge position of the sample was larger than that located in the core position of the billet. The core-sections of RUE formed billets were cut for taking the image and semi-solid processing.

AZ80 samples treated by RUE were cut into smaller pieces with 8 mm diameter \times 12 mm height cylinder samples for partial remelting experiments. The samples treated by RUE were heated into the semi-solid state in a vertical infrared tube furnace under protective gas flow (1% SF_6 in CO_2), isothermally held. A thermocouple placed in a hole of 3 mm diameter and 5 mm depth in the centre of the sample ensured accurate temperature measurement and feedback control. On removal from the furnace, the samples were immediately quenched in cold water.

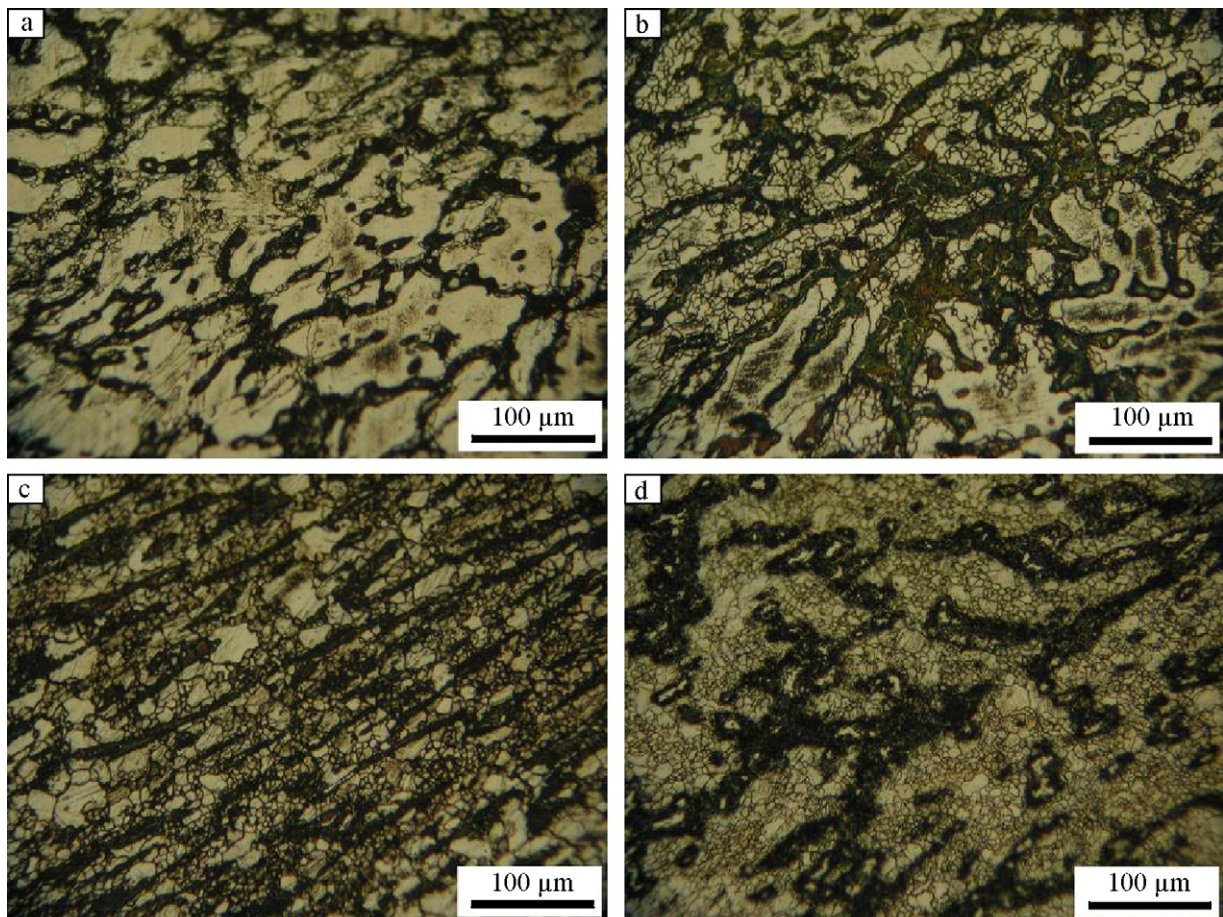


Fig. 5. Microstructure of RUE formed AZ80 magnesium alloy with different numbers of RUE passes: (a) two pass, (b) four passes, (c) six passes and (d) eight passes.

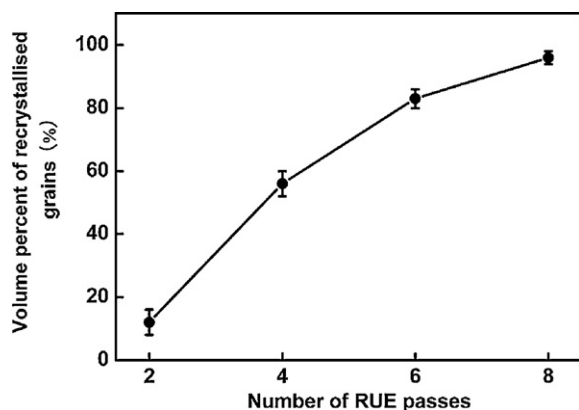


Fig. 7. Plot of volume percent of recrystallised grains as a function of number of RUE passes.

Thixoextrusion of barrel-shaped components was used to examine the thixoformability of RUE formed AZ80 magnesium alloy in the semi-solid state. The three-dimensional model of barrel-shaped component is shown in Fig. 2. As shown in Fig. 2, the barrel-shaped component belonged to the axisymmetrical component. It had three strengthening ribs with a width of 1.5 mm and a length of 120 mm in a lateral face.

Before the thixoextrusion, the RUE formed samples were machined into slugs with a diameter of 79 mm and a length of 120 mm. Argon was used as a gas environment (1% SF₆ in CO₂) to reduce oxidation during partial remelting. The diagrammatic sketch of forming die is shown in Fig. 3. The heating process was monitored by using two K-type thermocouples, located at a depth of 10 mm from the top of the slug, one in the centre and the other 8 mm from the outer surface, which were quickly extracted prior to thixoextrusion. Before the thixoextrusion, the die was heated to

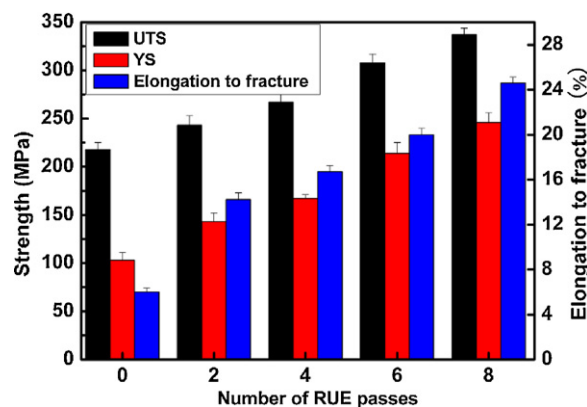


Fig. 8. Tensile mechanical properties of RUE formed AZ80 magnesium alloy with different numbers of RUE passes.

350 °C and oil-based graphite was used as a lubricant. The temperature and holding time of slug for thixoextrusion were chosen as 570 °C and 10 min, respectively. After the slug was held into the die, the slug was applied to the pressure of 400 MPa for 30 s. For comparison, cast AZ80 billets were also thixoextruded after partial remelting. After the thixoextrusion, barrel-shaped components were treated by blast sanding.

Preparation of metallographic samples consisted of grinding with SiC paper of different fineness and subsequently polishing with 1 μm diamond paste and colloidal 0.05 μm alumina. After ultrasonic cleaning in pure ethanol, the RUE formed samples were etched in a solution of 100 ml ethanol, 6 g picric acid, 5 ml acetic acid and 10 ml water. For as-cast and partially remelted samples, they were etched in a solution of 4% aqueous nitric acid. The dog bone-shaped tensile samples had a gauge length of 15 mm and a thickness of 2 mm. Tensile samples were tested using an Instron 5569 testing machine at a cross head speed of 1 mm min⁻¹. Each tensile

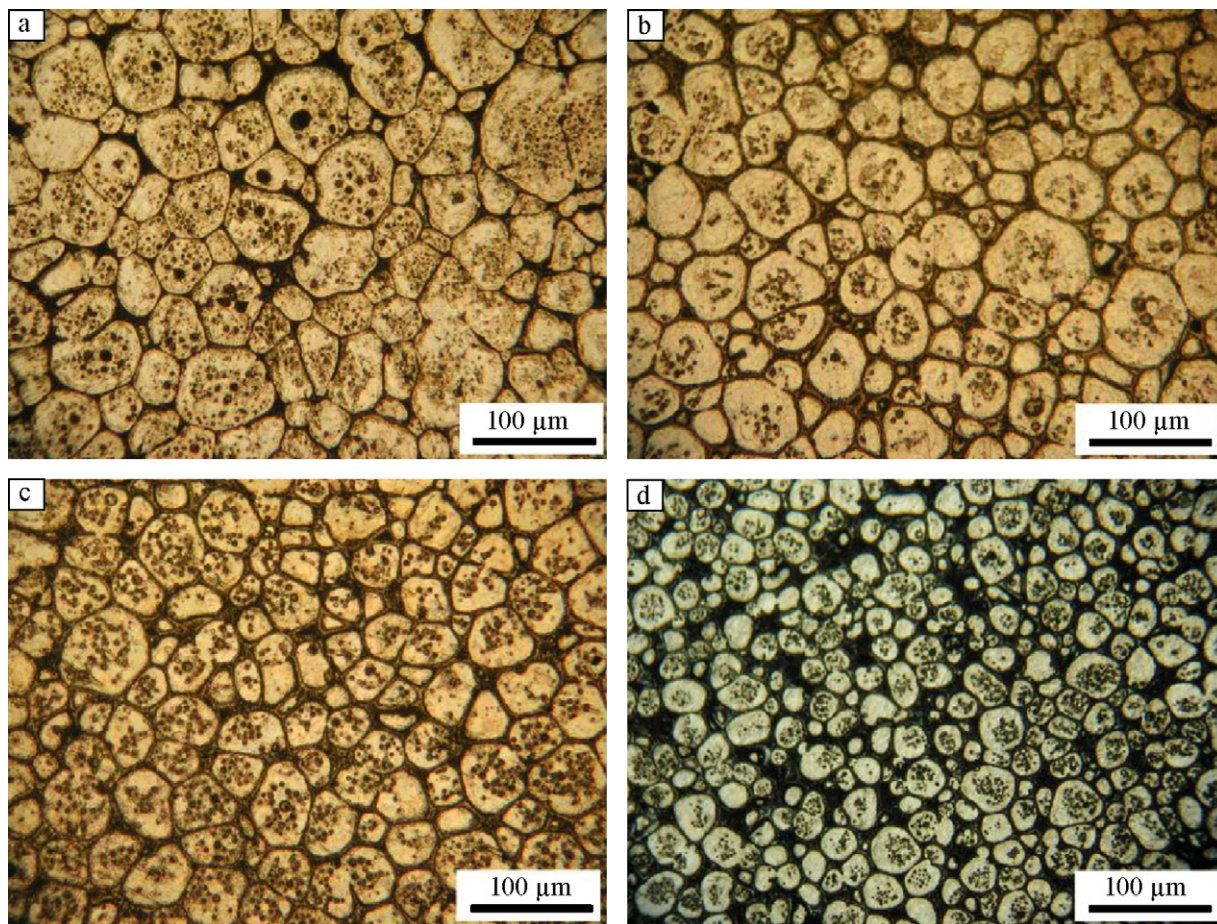


Fig. 9. Microstructure of RUE formed AZ80 magnesium alloy with different numbers of RUE passes: (a) two pass, (b) four passes, (c) six passes and (d) eight passes after partial remelting to 570 °C and 5 min isothermal holding.

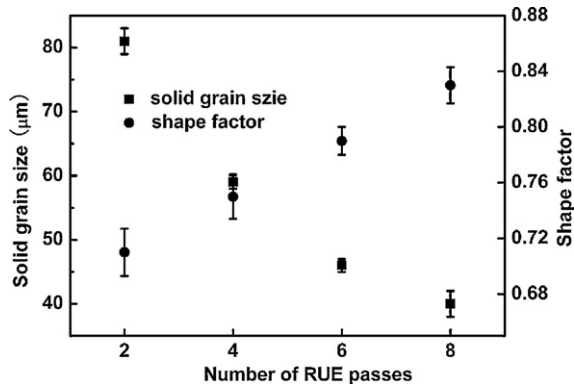


Fig. 10. Plot of solid grain size and shape factor of the RUE formed AZ80 magnesium alloy after partial remelting to 570 °C and 5 min isothermal holding as a function of number of RUE passes.

value was the average of at least five measurements. Mean size and shape factor of solid grains were calculated in each case by using Eqs. (3) and (4) [16].

$$d = \frac{\sum_{N=1}^N \sqrt{4A/\pi}}{N} \quad (3)$$

$$F = \frac{\sum_{N=1}^N (4\pi A)/P^2}{N} \quad (4)$$

where A and P are area and perimeter of solid particles respectively and N is the number of solid grains. For each sample, measurements were taken from the whole sectioned area with 200–300 solid particles per sample. Fracture cross sections were conducted with scanning electron microscopy (SEM).

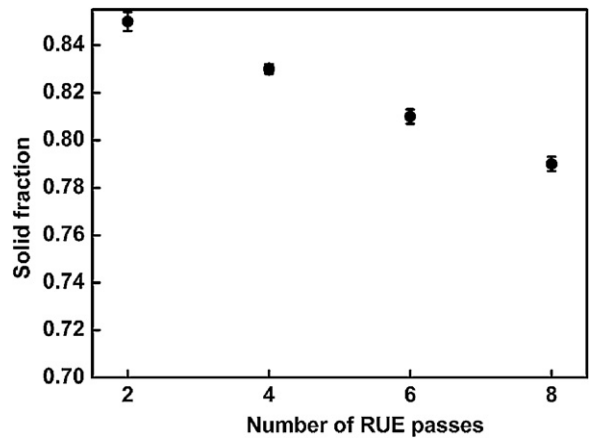


Fig. 11. Plot of solid fraction of the RUE formed AZ80 magnesium alloy after partial remelting to 570 °C and 5 min isothermal holding as a function of number of RUE passes.

3. Results

3.1. Microstructure and mechanical properties of RUE formed AZ80 magnesium alloy

Fig. 4 shows the microstructure of as-cast AZ80 magnesium alloy. The microstructure of as-cast AZ80 magnesium alloy consisted of α -Mg matrix and β -Mg₁₇Al₁₂ phase. The β -Mg₁₇Al₁₂ phase precipitated as discontinuous network at grain boundaries.

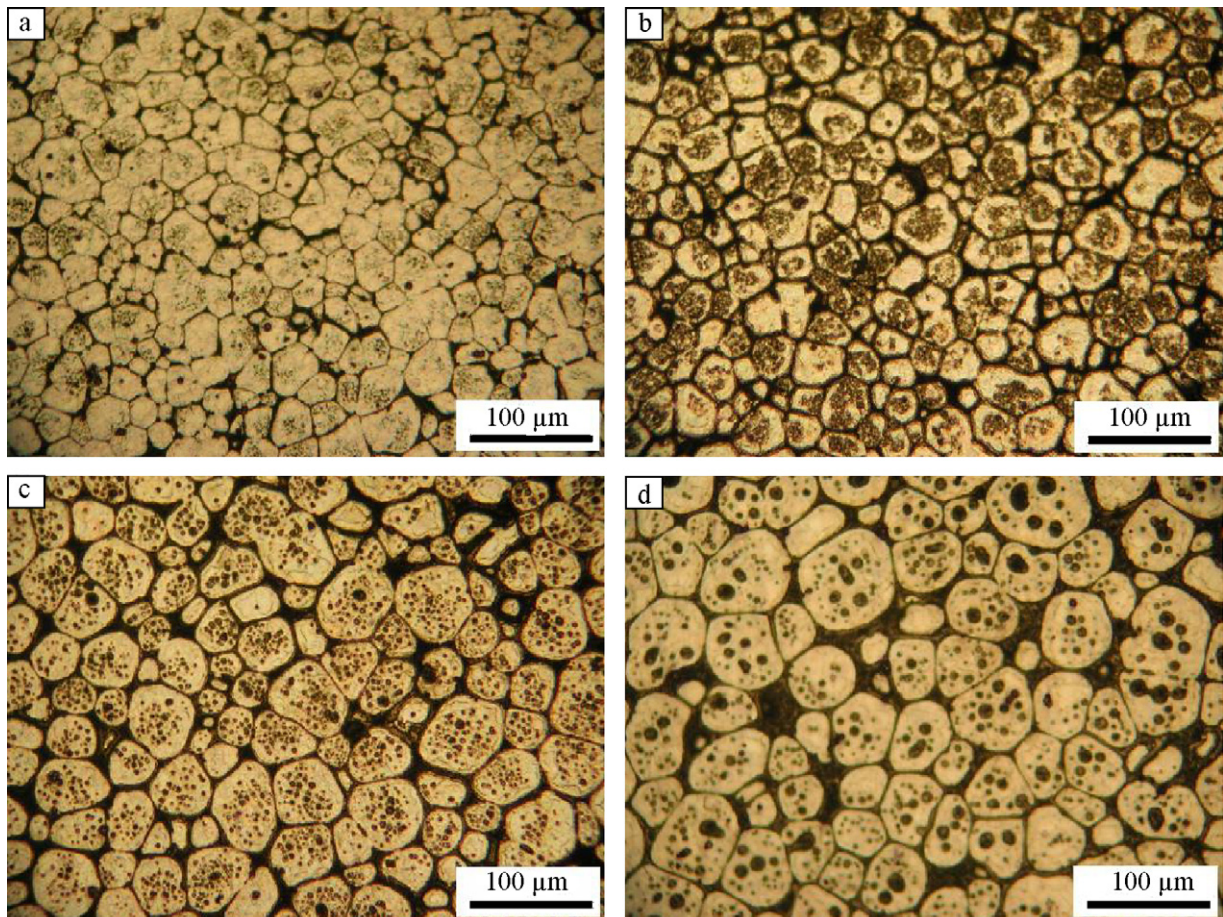


Fig. 12. Microstructure of eight-pass RUE formed AZ80 magnesium alloy reheated to 550 °C and isothermally held for (a) 5 min, (b) 10 min, (c) 20 min and (d) 30 min.

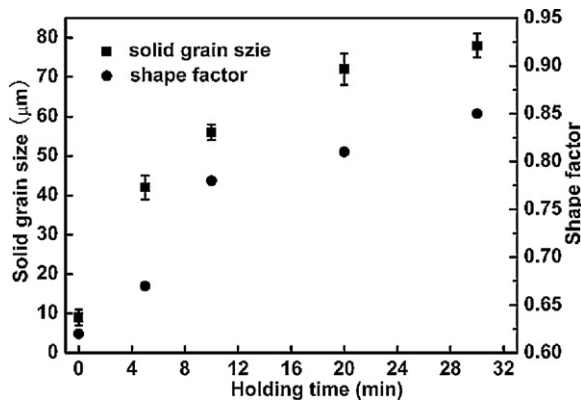


Fig. 13. Plot of solid grain size and shape factor of the eight-pass RUE formed AZ80 magnesium alloy after partial remelting to 550 °C for different holding times.

Fig. 5 shows the microstructure of RUE formed samples with different numbers of RUE passes. As shown in Fig. 5a, a large number of fine grains appeared at the initial grain boundaries, especially at triple junctions, when the sample was examined after two-pass RUE. When the coarse grains were examined more closely, it was found that many grain boundaries were serrated. Moreover, many fine grains were formed along the grain boundaries of coarse grains, which was a nucleation process typical for dynamic recrystallisation. When the number of RUE passes increased, non-recrystallised regions of old grains were still remained although the number of recrystallised grains was obviously increased (Fig. 5b). With further increase in the number of RUE passes, the area covered by fine grains increased and β -Mg₁₇Al₁₂ phase was obviously elongated along the deformation direction (Fig. 5c). When the number of RUE passes reached eight, the whole matrix of sample was taken up by new and recrystallised grains, which indicated that dynamic recrystallisation has been completed (Fig. 5d). Fig. 6 shows the evolution of mean grain size of RUE formed samples as a function of the number of RUE passes. As shown in Fig. 6, with increase in the number of RUE passes, the mean grain size of the RUE formed samples reduced. For example, the mean grain size decreased from 86 μm to 15 μm with the number of RUE passes increasing from two to six. However, with further increase in the number of RUE passes, the mean grain size changed a little. Generally, the as-cast AZ80 magnesium alloy formed at low degree of deformation presented more efficient improvement of grain refinement. The grain size decreased rapidly with increasing the number of RUE passes and then it was little influenced by increasing the number of RUE passes on certain conditions. Fig. 7 shows plot of volume percent of recrystallised grains as a function of number of RUE passes. As shown in Fig. 7, the variation curve was parabolic, which meant higher growth rate of volume percent of recrystallised grains at lower degree of deformation and lower growth rate at greater degree of deformation. Fig. 8 shows the influence of number of RUE passes on tensile mechanical properties of as-cast AZ80 magnesium alloy. The results indicated that the ultimate tensile strength (UTS), yield strength (YS) and elongation to fracture increased with the number of RUE passes. For example, the UTS, YS and elongation to fracture of the as-cast AZ80 magnesium alloy increased from 218 MPa, 103 MPa and 6.1% to 337 MPa, 246 MPa and 24.6%, respectively, when the number of RUE passes increased from zero to eight.

3.2. The effect of number of RUE passes on the microstructure of RUE formed AZ80 magnesium alloy in the semi-solid state

Fig. 9 shows the semi-solid microstructure of RUE formed AZ80 magnesium alloys with different numbers of RUE passes followed by heating for 5 min holding at 570 °C. Following partial remelt-

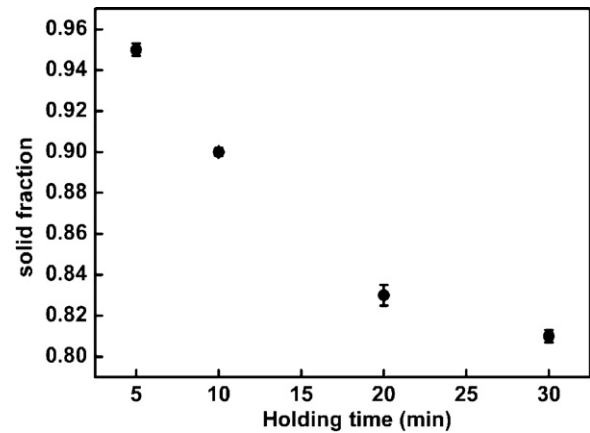


Fig. 14. Plot of solid fraction of the eight-pass RUE formed AZ80 magnesium alloy after partial remelting to 550 °C for different holding times.

ing in each case, the microstructure consisted of solid grains with a liquid film and solid grains were well globularized (Fig. 9). With increase in the number of RUE passes, the solid grain size obviously decreased and the shape became more spheroidal (Fig. 10). Moreover, the amount of liquid increased with the number of RUE passes (Fig. 11).

3.3. The effect of isothermal holding time and temperature on the microstructure of RUE formed AZ80 magnesium alloy in the semi-solid state

Fig. 12 shows microstructure of the eight-pass RUE formed AZ80 magnesium alloy partially remelted at 550 °C for different holding times. When heated to 5 min, banded structures (β -Mg₁₇Al₁₂ phase) in the microstructure disappeared and liquid pools appeared in certain areas. Conglomerated structures were also separated into individual solid grains because of liquid penetration. Although most of solid grains were irregular in shape, some solid grains surrounded by liquid had undergone a significant degree of spheroidization (Fig. 12a). When the holding time was extended to 10 min, parts of the edges of polygonal solid grains melted, which resulted in the spheroidization of polygonal solid grains and the increase in the amount of liquid phase. Moreover, close examination of the microstructure (Fig. 12b) revealed that solid grains had undergone coarsening by coalescence, because these neighboring solid grains had a perfectly matching crystallographic orientation. As the holding time was prolonged, solid grains coarsened and the degree of spheroidization was improved. Simultaneously, liquid was gathered in pools and some small solid grains suspended in

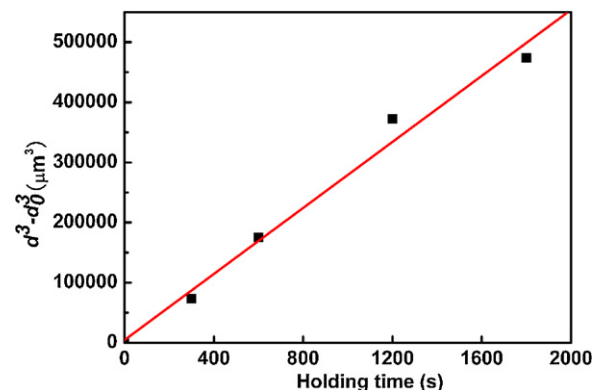


Fig. 15. Plot of $d^3 - d_0^3$ for eight-pass RUE formed AZ80 magnesium alloy reheated at 550 °C as a function of holding time.

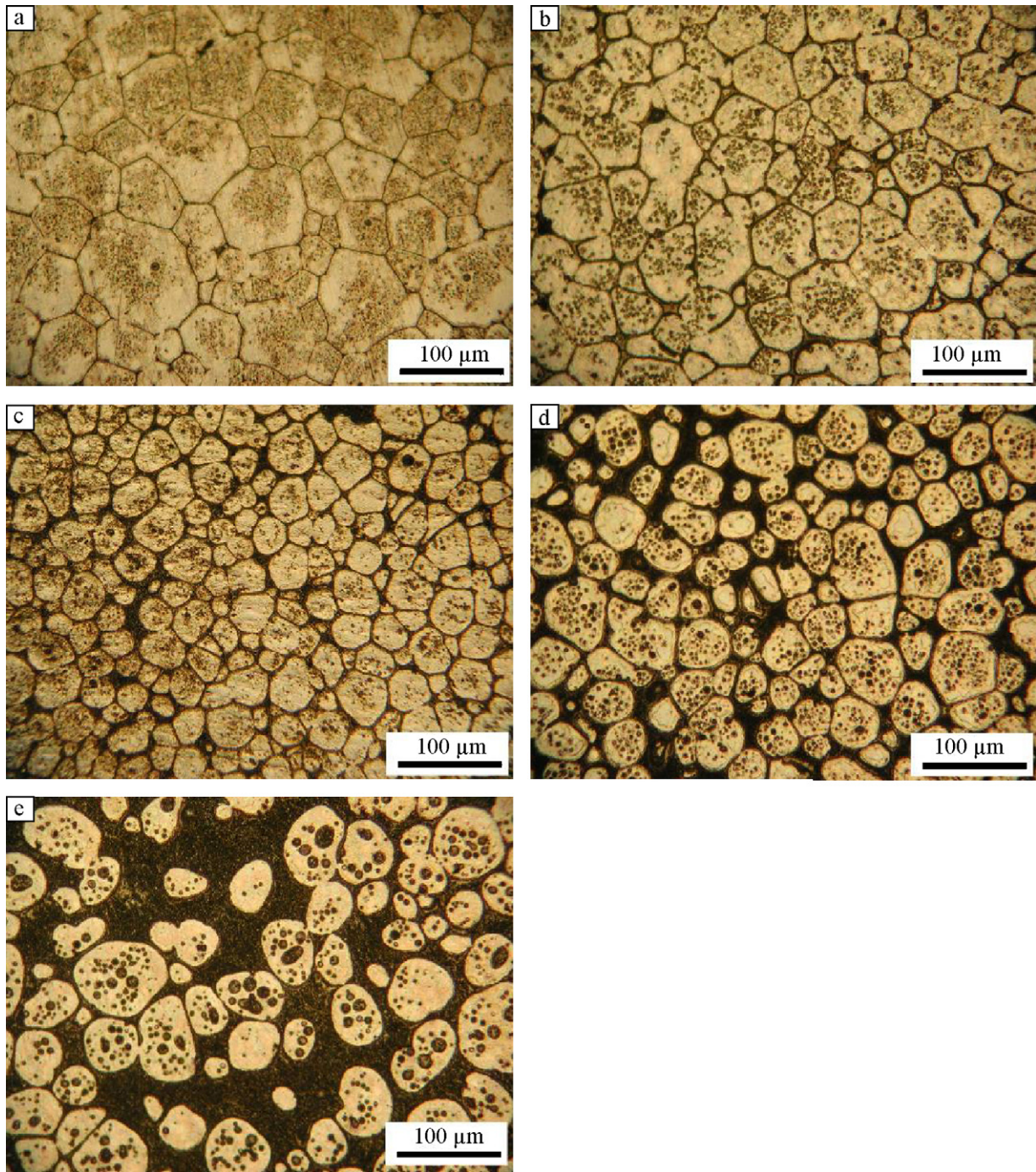


Fig. 16. Microstructure of eight-pass RUE formed AZ80 magnesium alloy partially remelted at (a) 540 °C, (b) 550 °C, (c) 560 °C, (d) 570 °C and (e) 580 °C for 10 min isothermal holding.

liquid pools (Fig. 12c). When the holding time was extended to 30 min, a key feature of the microstructure was entrapped liquid pools in the interior of solid grains. It was also interesting to observe that isolated solid grains suspending in the liquid pools had a grain size much smaller than that of the majority of the aggregated solid grains (Fig. 12d). Fig. 13 shows that the results from the microstructure evolution as a function of the holding time in the semi-solid state for the eight-pass formed AZ80 magnesium alloy. Solid grains in the eight-pass formed AZ80 magnesium alloy coarsened during isothermal holding, while the degree of spheroidization was improved. Fig. 14 shows the solid fraction was decreased with prolonging holding time.

In the theory of Ostwald ripening, the time dependency of the size of a growing solid grain can be described by the classical LSW relationship [17]:

$$d^n - d_0^n = Kt \quad (5)$$

where d_0 is the initial grain size, d is the size at time t , K is the coarsening rate constant and n is the coarsening exponent. The experimental results and the linear regression curves from Eq. (5) is shown in Fig. 16. The resulted R^2 value (0.99264) was very close to 1, indicating that the experimental data were well fitted to the LSW equation at $n = 3$. The cubic coarsening rate constant, K , in Eq. (5) was given experimentally by the gradient of the best fit straight

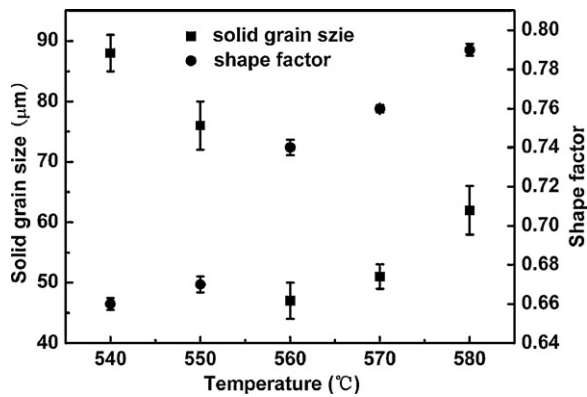


Fig. 17. Plot of solid grain size and shape factor of the eight-pass RUE formed AZ80 magnesium alloy after partial remelting to (a) 540 °C, (b) 550 °C, (c) 560 °C, (d) 570 °C and (e) 580 °C for 10 min isothermal holding.

lines shown in Fig. 15 and was $248 \mu\text{m}^3 \text{s}^{-1}$ for the sample treated by eight-pass RUE after partial remelting.

Fig. 16 shows microstructure of eight-pass RUE formed AZ80 magnesium alloy partially remelted at different temperatures for 10 min isothermal holding. As shown in Fig. 16, the microstructure consisted of solid grains surrounded by liquid. When the temperature increased from 540 °C to 560 °C, the solid grain size decreased initially, and then the solid grain size increased with further increasing temperature (Fig. 17). Fig. 18 shows that the amount of liquid phase increased with increasing temperature.

3.4. Thixoextrusion and mechanical properties of thixoextruded AZ80 magnesium alloy prepared by RUE

From the results of the partial remelting experiments, a suitable temperature for thixoextrusion the RUE formed AZ80 magnesium alloy samples with a diameter of 8 mm and a length of 12 mm appeared to be at 570 °C for 5 min isothermal holding (Fig. 9d). However, it was found in practice that it was almost impossible to obtain homogeneous spheroidal solid grains with a liquid film in the RUE formed samples due to the 'skin effect' phenomenon. The inside of the slug with a diameter of 79 mm and a length of 120 mm heated up more slowly via thermal conduction from the hotter surface. Therefore, proper prolonged holding time to 10 min was feasible to obtain the homogeneous microstructure. Fig. 19 shows five fingers thixoextruded at 100 mm s⁻¹ ram speed (die filling velocity), 30 s dwell, at the temperature of 570 °C for 10 min

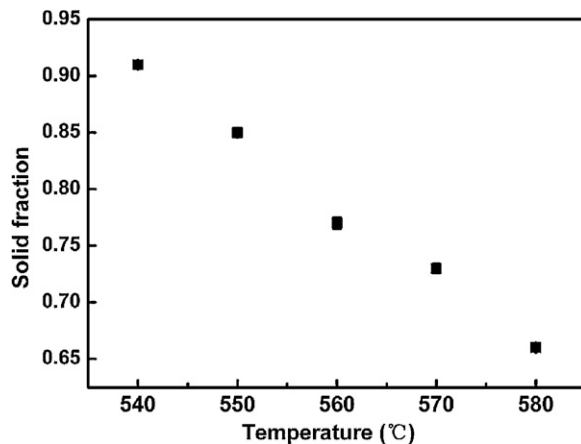


Fig. 18. Plot of practical solid fraction of the eight-pass RUE formed AZ80 magnesium alloy after partial remelting to (a) 540 °C, (b) 550 °C, (c) 560 °C, (d) 570 °C and (e) 580 °C for 10 min isothermal holding.



Fig. 19. Barrel-shaped components thixoextruded from eight-pass RUE formed AZ80 magnesium alloy.

isothermal holding from a cylindrical slug of 79 mm diameter by 120 mm height. The reproduction of the barrel-shaped component was shown to be good, and no problem was experienced in filling the rib sections. Fig. 20 shows the tensile mechanical properties of AZ80 components thixoextruded from as-cast and eight-pass RUE formed alloy. The results show that the mechanical properties of AZ80 components thixoextruded from eight-pass RUE formed alloy were better than those thixoextruded from as-cast alloy. Moreover, the mechanical properties of thixoextruded components obtaining from the bottom part were better than those obtaining from the lateral part.

The microstructure features across the mid-section of components thixoextruded after reheating in the semi-solid temperature range, from as-cast and eight-pass RUE formed AZ80 magnesium alloys are shown in Figs. 21 and 22, respectively. As shown in Fig. 21, the former exhibited a coarse and heterogeneous structure. The component thixoextruded from RUE formed alloy, on the other hand, exhibited ideal and fine semi-solid microstructure, in which completely globular primary phase solid grains had little amount of intragranular liquid droplets (Fig. 22). It was also noteworthy that the solid grain size of bottom part was slightly smaller than that of lateral part in components thixoextruded starting from as-cast and RUE formed AZ80 magnesium alloys. Typical SEM micrographs for components thixoextruded from as-cast and RUE formed alloys are shown in Figs. 23 and 24. Obviously, there was no evidence of plastic deformation and the fracture surfaces exhibited a typical brittle rupture in the components thixoextruded from as-cast alloy (Fig. 23a and b). A detail view of this type of failure is shown in

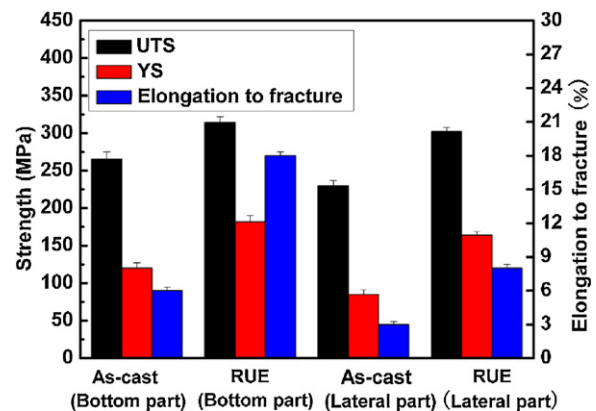


Fig. 20. Tensile mechanical properties of thixoextruded components starting from as-cast and eight-pass RUE formed AZ80 magnesium alloy.

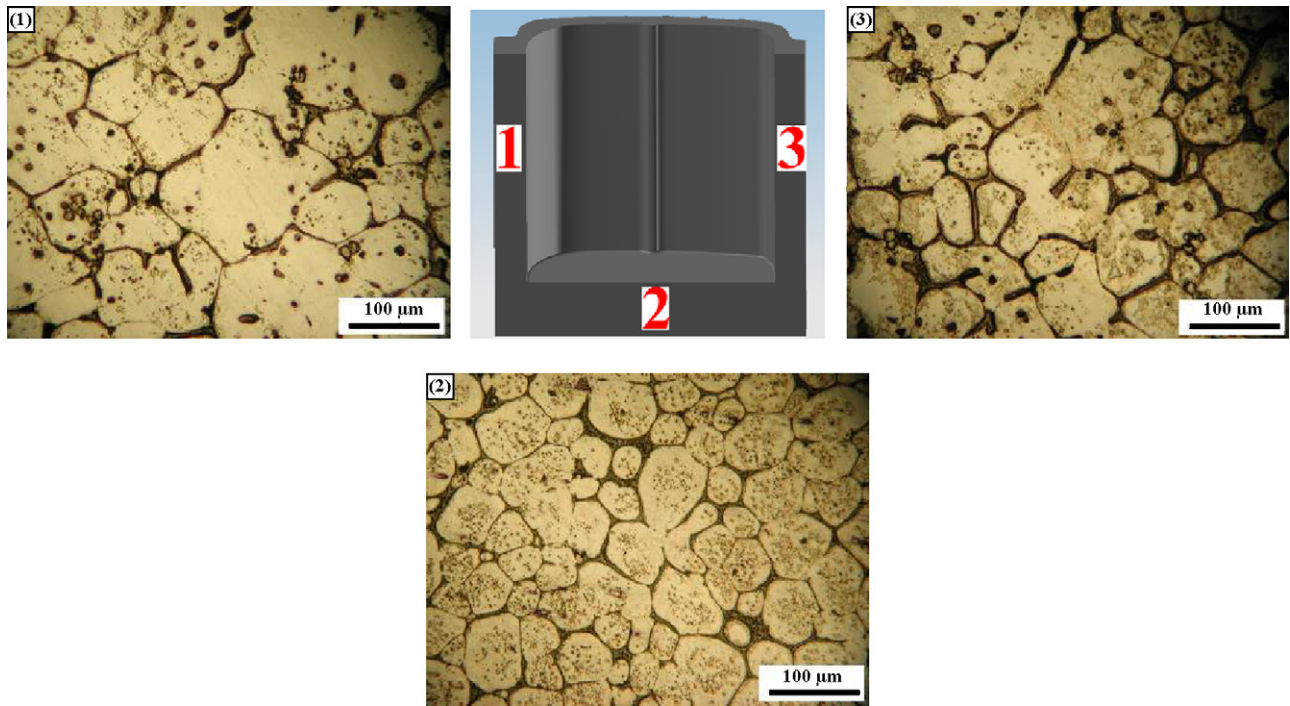


Fig. 21. Optical micrographs from different locations on the mid-section of the component thixoextruded from as-cast AZ80 magnesium alloy.

Fig. 24, revealing the interface morphology with a crack penetrating along the α -Mg and $Mg_{17}Al_{12}$ intermetallic compound. However, the fracture surfaces of the components thixoextruded from RUE formed alloy illustrate the high ductility (Fig. 23c and d). The tensile fracture surfaces mainly consisted of a large number of dimples and tear ridges, which indicated that significant plastic deformation occurred.

4. Discussion

4.1. Microstructure evolution and mechanical properties of RUE formed AZ80 magnesium alloy

From the results presented in Figs. 5–7, the effect of number of RUE passes on the microstructure of RUE formed AZ80 magne-

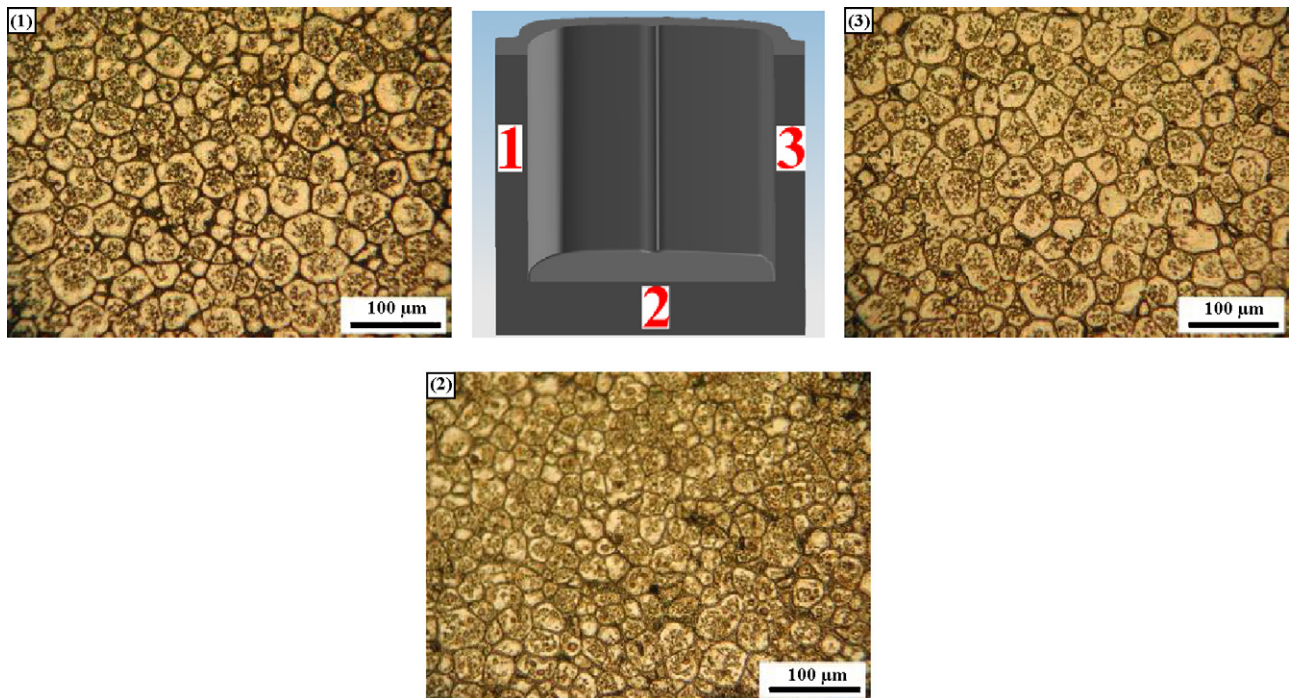


Fig. 22. Optical micrographs from different locations on the mid-section of the component thixoextruded from RUE formed AZ80 magnesium alloy.

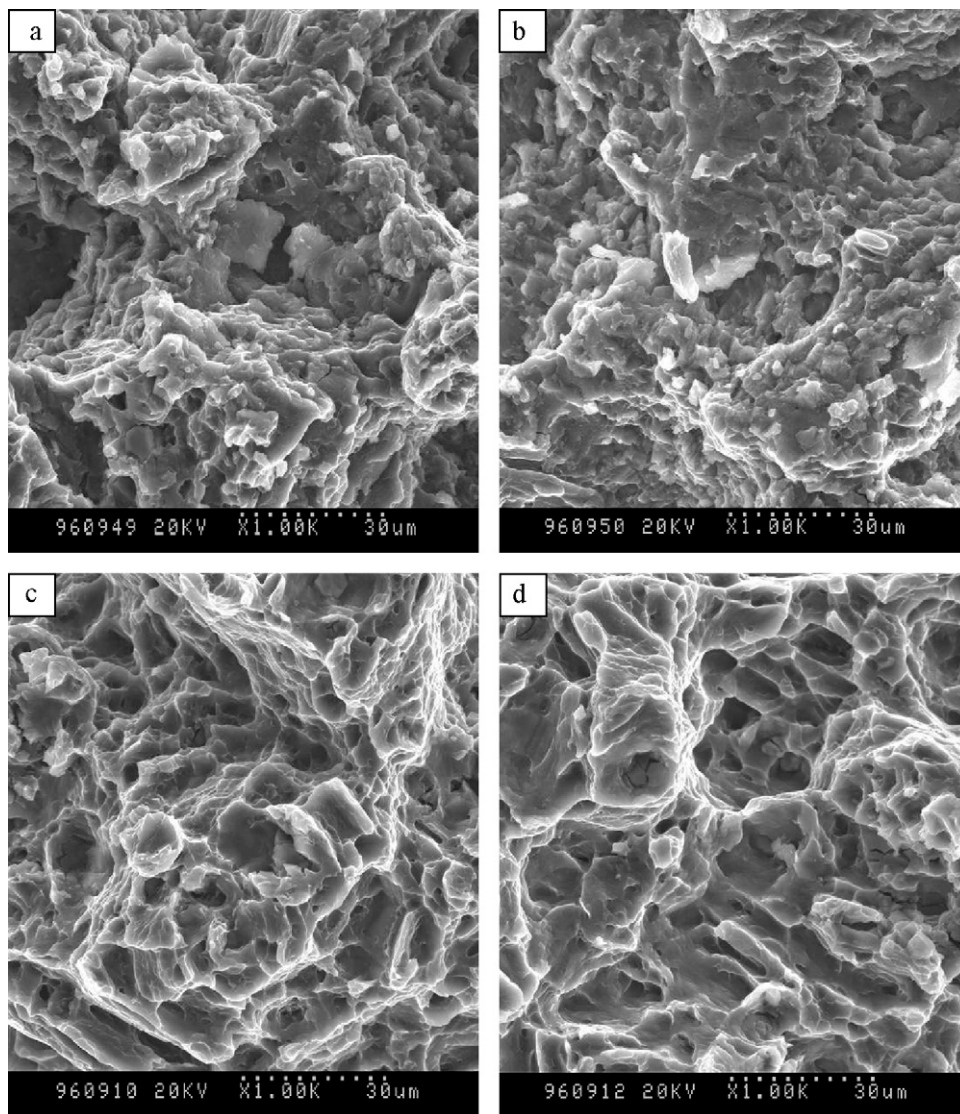


Fig. 23. SEM image of ruptured surfaces of tensile samples after thixoextrusion in different positions of components: (a) as-cast alloy (lateral part), (b) as-cast alloy (bottom part), (c) RUE formed alloy (lateral part) and (d) RUE formed alloy (bottom part).

sium alloy could be summarized as: (a) fine grains were generated immediately after two-pass RUE. With increasing number of RUE passes, the number of fine grains increased and the mean grain size decreased, (b) the grain shape became more equiaxed-like, and (c) the recrystallised grains were heterogeneously generated mainly from coarse grain boundaries. As clearly shown in Fig. 5a, the discovery of the nucleation of fine grains at original coarse grain boundaries indicated that dynamic recrystallisation occurred. The driving force for dynamic recrystallisation was associated with the excess energy stored in the crystal as a result of RUE [18]. With increasing number of RUE passes, recrystallised fine grains replaced the original coarse grains. Comparison of Fig. 5a–d indicates the alloy formed by more numbers of RUE passes gave a finer recrystallised grain size. The more the numbers of RUE passes, the greater the overall grain boundary and sub-grain boundary area. This led to greater potential for the development of recrystallisation nuclei, and therefore a finer recrystallised grain size. Increasing the amount of deformation increased the driving force for recrystallisation, since a heavily deformed sample contained more stored energy necessary for the recrystallisation process. Compared with direct extrusion, the alloy treated by RUE could obtain the smaller

solid grain size during partial remelting at the same thermodynamic process. Kleiner et al. [19] suggested that the solid grain size of AZ80 alloy treated by direct extrusion with an equivalent strain of 2.35 after 5 min holding at 570 °C was about 80 μm. However, in the present study, the solid grain size of AZ80 alloy treated by RUE with an equivalent strain of 2.68 after 5 min holding at 570 °C was only about 46 μm.

For AZ80 magnesium alloy, the main strengthening intermetallic was $Mg_{17}Al_{12}$ phase. The body-centered cubic (b.c.c.) structure of $Mg_{17}Al_{12}$ was incompatible with the h.c.p. structure of magnesium matrix, which resulted in the fragility of the Mg/ $Mg_{17}Al_{12}$ interface. In addition, $Mg_{17}Al_{12}$ itself was relatively soft and had poor strength. Therefore, microcracks tended to initiate in the Mg/ $Mg_{17}Al_{12}$ interface and even in the particles. The volume and morphology of $Mg_{17}Al_{12}$ greatly influenced the mechanical properties of AZ80 alloy. After RUE, band structures appeared in the microstructure. Band structures were typical for extruded products of magnesium–aluminum alloys. These band structures consisted of $Mg_{17}Al_{12}$ phase. Because of non-equilibrium freezing, as-cast AZ80 magnesium alloy billets had gross segregation. During RUE, $Mg_{17}Al_{12}$ was partially dissolved. However, time was too short to

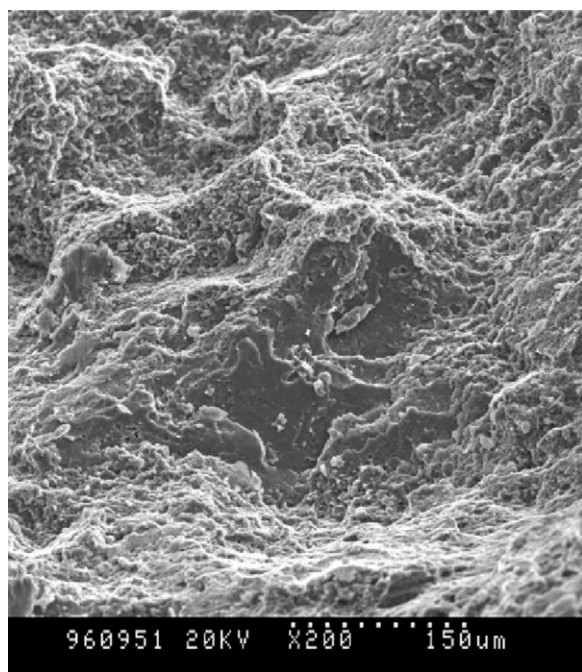


Fig. 24. SEM image of thixoextruded components from as-cast AZ80 magnesium alloy (lateral part).

allow complete homogenization during RUE and segregation was only reduced and elongated but not eliminated. On cooling from the extrusion temperature, precipitation of lamellar $\text{Mg}_{17}\text{Al}_{12}$ occurred only in the areas of higher Al-content [19].

The tensile mechanical properties of RUE formed AZ80 magnesium alloy exhibited a general tendency where an increase in the number of RUE passes caused an increase in strength and ductility (Fig. 8). Moreover, higher strength values corresponded to larger elongation to fracture. As the number of recrystallised grains increased and grain size became smaller, dislocations within each grain could travel a smaller distance before they encountered the grain boundary, at which point their movement was terminated (dislocation pile up). It was for this reason that fine-grained alloy possessed a higher mechanical properties according to the Hall–Petch relation.

4.2. Microstructure evolution of RUE formed AZ80 magnesium alloy during partial remelting

During the initial stage of partial remelting, because the temperature increased in the RUE formed alloy, the $\beta\text{-Mg}_{17}\text{Al}_{12}$ dissolved into the primary α -grains, which resulted in the increase of Al content in the primary α -grains. Because the increase of temperature in the sample was too rapid that there was not enough time for the $\beta\text{-Mg}_{17}\text{Al}_{12}$ to completely dissolve into the primary α -grains. And then the residual $\beta\text{-Mg}_{17}\text{Al}_{12}$ phase began to melt. As the holding time is further prolonged, the amount of liquid phase increased because of melting of primary α -grains. Tzimas and Zavaliangos [20] suggested that grain coalescence and Ostwald ripening operated simultaneously and independently as soon as liquid was formed. At short times, the distance between neighboring solid grains was short and the thickness of solid grain boundary liquid films was thin (Fig. 12a). Solid grains were partially interconnected by un-wetted grain boundaries and some liquid filled the intergranular spaces. Therefore, the solid grain coarsening behavior was controlled mainly by coalescence. With prolonged holding time, the amount of liquid

increased (Fig. 12b). The coalescence was less active, because at higher liquid contents, the probability that solid grains would come in contact with each other, was decreased. Therefore, after a long time holding, the dissolution–reprecipitation diffusion-controlled mechanism was the dominant growth mechanism. However, too long isothermal holding unavoidably led to excessive grain growth, which in turn impaired both the subsequent rheological behavior of the semi-solid alloy and the mechanical properties of the component formed (Figs. 12d and 13). The degree of spheroidization strongly depended on spheroidizing driving force, which was governed by the Gibbs–Thompson effect. To reduce interfacial energy between solid grains and liquid matrix, the diffusional transport of the material occurred and the solid grains gradually became spheroidal. As the amount of liquid increased, the corners and edges of the solid grains would melt, the distance between particles increased due to the increase of liquid phase and thus the probability of the merging decreased [2]. Therefore, solid grain gradually became spheroidal (Fig. 14).

When reheating at a relative low temperature, the distance between adjacent solid grains was short because of the limited amount of liquid. Therefore, the probability of solid grain coalescence should be greater, which led to the larger solid grain size at low temperature (Fig. 16a). Since the number of neighboring solid grains decreased with increasing volume fraction of liquid, it was expected that Ostwald ripening was dominant at high volume fractions of liquid and solid grains size decreased. However, the role of Ostwald ripening could be greater because of faster diffusion at high temperatures. Therefore, solid grain size increased and the degree of spheroidization was improved with further prolonged holding time. The comparison of grain size between the RUE formed alloy (Fig. 5) and partial remelted alloy (Fig. 9) indicated that the solid grain size depended on the number of RUE passes. The more the number of RUE passes, the smaller the recrystallised grains and the smaller the solid grain size. In other words, the solid grain size in the semi-solid state inherited from recrystallised grain size. It was also noteworthy that too long holding time (Fig. 12d) and too low temperature (Fig. 16a) caused excessive grain coarsening, which weakened the effect of the number of RUE passes on solid grain size. Moreover, with increase in number of RUE passes, the rate of liquid formation enhanced. The more the numbers of RUE passes, the greater the overall recrystallised grain boundary. When the temperature increased to above solidus, the alloy treated by more the numbers of RUE passes possessed much solid-liquid interfacial energy that that by few passes. With increasing solid-liquid interfacial energy, diffusion rate increased, which in turn enhanced the rate of liquid formation. The significant difference in the degree of spheroidization among the RUE formed alloy with different numbers of RUE passes after partial remelting should be delineated. The faster kinetics of spheroidization observed in alloy treated by more numbers of RUE passes was attributed to the equiaxed shape in the original microstructure, a smaller recrystallised grain size, and thus smaller diffusion distances required for spheroidization and more interfacial surface energy. Therefore, more numbers of RUE passes and a finer grained microstructure should promote a faster spheroidization in the alloy treated by more numbers of RUE passes (Fig. 10).

Intragranular liquid droplets were present in alloys during partial remelting, as shown in Figs. 9, 12 and 16. Plenty of very small intragranular liquid droplets developed in the early stage of partial remelting (Fig. 12a). These small intragranular liquid droplets became fewer but bigger with increasing holding time in the semi-solid state by minimizing the solid-liquid surface (Fig. 12d). Finally, at long times it was expected that the amount of intragranular liquid droplets decreased by migration to liquid matrix by diffusion

through the solid phase driven by the minimization of solid–liquid interface within the grain, provided that no further coalescence [20].

4.3. Microstructure and mechanical properties of components thixoextruded starting from as-cast and RUE formed AZ80 magnesium alloys

Thixoextrusion was the shaping of metal components in the semi-solid state. The processing temperature was between the solidus and liquidus. The nucleation and solidification of eutectic liquid after forming was an important factor for thixoextrusion to obtain the ideal microstructure with good mechanical properties [21]. Moreover, the mechanical properties of thixoextruded components depended on the quality of feedstock and thermodynamic parameters (holding time and temperature). As discussed above, the material with fine and equiaxed grains was favorable for obtaining the ideal semi-solid microstructure, in which spheroidal solid grains were dispersed in liquid matrix. The good microstructure features of the component thixoextruded from starting material treated by RUE were attributed to fine recrystallised grains before partial remelting. Deformation introduced by RUE was favorable for obtaining small globular solid grains surrounded by liquid. However, on the other hand, the as-cast alloy undergone obvious coarsening. The heterogeneous solid grain structure with some very coarse grains thus obtained was clearly not as thixoformable as the RUE formed alloy. Fig. 20 shows considerable improvement in the mechanical properties of components thixoextruded from the RUE formed alloy over those of components thixoextruded from the as-cast alloy. The RUE formed alloys treated by partial remelting were free porosity, and had a homogeneous microstructure. This in turn resulted in higher strengths and elongation to fracture in the components thixoextruded from the RUE formed alloys compared with components thixoextruded from the as-cast alloys. Moreover, the transcrystalline cracking of the solid grains was the main fracture mechanism in the components thixoextruded from the RUE formed alloys. In contrast, decohesion at the interface between the eutectic and the solid grain was predominant in components thixoextruded from the as-cast alloys. Comparison of Figs. 8 and 20 indicate that the mechanical properties of components thixoextruded from the RUE formed alloy did not achieve the quality of RUE formed alloy. It was believed that the mechanical properties of thixoformed parts depended on the microstructure before thixoforming. Long isothermal holding time would result in excessive grain growth and thus poor mechanical properties in the final component. In the present study, after 10 min isothermal holding, solid grains slightly coarsened and spheroidal solid grains were dispersed in the liquid matrix. Moreover, with prolonged holding time, the feature of decohesion at the interface between the eutectic and α -Mg was more obvious. Therefore, the mechanical properties of thixoformed parts were slightly lower than those of RUE formed billets.

It was interesting to note that the mechanical properties of components in the bottom part were better than those in the lateral part (Fig. 20). Careful examination of the thixoformed microstructure indicated the deformation was mainly achieved by sliding among solid grains and slight plastic deformation of the solid grains (Figs. 21 and 22). The deformation force required was to overcome the friction generated from the sliding between solid grains, and to overcome the restriction of the solid grain movement due to the spatial constraint imposed by the surrounding solid grains, and also yield strength of solid grains. After mould filling, solidification in the die cavity occurred. Inside the die cavity, the remaining liquid had uniform temperature and composition fields. An applied pressure increased the melting temperature for

magnesium alloys. Moreover, under the pressure exerted by the ram, the microstructure was compacted. Although zones 1 and 2 were the major deforming zones with 3D compressive stress. However, the absolute value of 3D compressive stress in zone 2 was higher than that in zone 1, because 3D compressive stress in zone 2 was supplied by the ram and 3D compressive stress in zone 1 was supplied by the frictional force. The greater value of 3D compressive stress was favorable for the compaction of materials. Moreover, greater 3D compressive stress promoted the solidification process, which in turn inhibited solid grain coarsening. Therefore, better mechanical properties were obtained in zone 2.

The liquid–solid segregation phenomenon during semi-solid deformation mainly depended on the deformation mechanism. Chen and Tsao [22] suggested that as the solid fraction decreased, the liquid flow mechanism and the flow of liquid incorporating mechanism were dominant. Under these conditions, the solid grains segregated in the centre portion, while the liquid segregated around the edge. However, with the increase of solid fraction, the deformation was achieved by sliding among solid grains. Under this condition, during the semi-solid processing, the liquid–solid segregation due to variation of pressure in the die could be restrained. Careful observation of optical microstructure of the component thixoextruded from RUE formed AZ80 magnesium alloy indicated that the deformation was achieved by sliding among solid grains and the liquid–solid segregation phenomenon had not been observed (Fig. 22).

5. Conclusions

1. The repetitive upsetting-extrusion process is successfully applied to predeform as-cast AZ80 magnesium alloy in the SIMA route. The fine grain has been obtained, and both the strength and ductility of the alloy are improved significantly after eight-pass RUE.
2. Repetitive upsetting-extrusion following by partial remelting is an effective method to produce semi-solid AZ80 magnesium alloy slugs for thixoextrusion. The process has been shown to produce ideal, fine semi-solid microstructures, in which completely spheroidal primary solid grains have intragranular liquid droplets. An ideal semi-solid microstructure with spheroidal solid grains can be obtained when the as-cast AZ80 magnesium alloy is subjected to eight-pass repetitive upsetting-extrusion and then is heated at 570 °C for 5 min.
3. With increasing the number of repetitive upsetting-extrusion passes, the solid grain size decreased and the degree of spheroidization was improved during partial remelting. At the same time, the rate of liquation was also improved. Prolonged holding time resulted in grain coarsening and the improvement of degree of spheroidization. Proper increase in temperature was favorable for obtaining semi-solid microstructure with small and spheroidal solid grains. Liquid was also present during partial remelting as fine intragranular droplets. These droplets were larger at higher temperature or for long time isothermal holding, and became less numerous as partial remelting progressed. The variation of the solid grains with holding time obeys the LSW law.
4. AZ80 magnesium alloy prepared by the SIMA route (repetitive upsetting-extrusion plus partial remelting) can be thixoextruded. The tensile properties for AZ80 magnesium alloy thixoextruded from starting material produced by RUE are better than those of AZ80 magnesium alloy thixoextruded from starting material produced by casting.

Acknowledgements

We are grateful for the support of the National Natural Science Foundation of China (NSFC) for support under Grant No. 51005217. Dr. Chen is grateful for the support from China Postdoctoral Science Foundation Grant No. 20100480677.

References

- [1] T.J. Chen, X.D. Jiang, Y. Ma, Y.D. Li, Y. Hao, J. Alloys Compd. 505 (2010) 476–482.
- [2] T.J. Chen, X.D. Jiang, Y. Ma, Y.D. Li, Y. Hao, J. Alloys Compd. 497 (2010) 147–154.
- [3] Y. Wang, G. Liu, Z. Fan, Acta Mater. 54 (2006) 689–699.
- [4] J. Hana, A. David, M. Bohuslav, J. Alloys Compd. 504S (2010) S500–S503.
- [5] H.V. Atkinson, K. Burke, G. Vaneetveld, Mater. Sci. Eng. A490 (2008) 266–276.
- [6] S. Chayong, H.V. Atkinson, P. Kapranos, Mater. Sci. Eng. A390 (2005) 3–12.
- [7] D. Liu, H.V. Atkinson, P. Kapranos, W. Jirattiticharoean, H. Jones, Mater. Sci. Eng. A 361 (2003) 215.
- [8] H.V. Atkinson, D. Liu, Mater. Sci. Eng. A 496 (2008) 439–446.
- [9] H.V. Atkinson, Prog. Mater. Sci. 50 (2005) 346–354.
- [10] T. Aizawa, K. Tokumitsu, Mater. Sci. Forum 312–314 (1999) 13.
- [11] L.X. Hu, Y.P. Li, E.D. Wang, Y. Yang, Mater. Sci. Eng. A 422 (2006) 327–332.
- [12] S. Ashouri, M. Nili-Ahmadabadi, M. Moradi, M. Iranpour, J. Alloys Compd. 466 (2008) 67–72.
- [13] T.J. Chen, G.X. Lu, Y. Ma, Y.D. Li, Y. Hao, J. Alloys Compd. 486 (2009) 124–135.
- [14] M. Moradi, M. Nili-Ahmadabadi, B. Poorganji, B. Heidarian, M.H. Parsa, T. Furuharac, Mater. Sci. Eng. A 527 (2010) 4113–4121.
- [15] M.C. Fleming, Solidification Processing, McGraw Hill, 1974, pp. 160–161.
- [16] F. Czerwinski, A. Zielinska-Lipiec, P.J. Pinet, J. Overbeeke, Acta Mater. 49 (2001) 1225–1235.
- [17] B. Nami, S.G. Shabestari, S.M. Miresmaeili, H. Razavi, Sh. Mirdamadi, J. Alloys Compd. 489 (2010) 570–575.
- [18] S.X. Ding, C.P. Chang, P.W. Kao, Met. Mater. Trans. A 40 (2009) 415–425.
- [19] S. Kleiner, O. Beffort, P.J. Uggowitzer, Scripta Mater. 51 (2004) 405–410.
- [20] E. Tzimas, A. Zavaliangos, Mater. Sci. Eng. A289 (2000) 228–240.
- [21] D. Liu, H.V. Atkinson, P. Kapranos, H. Jones, J. Mater. Sci. 39 (2004) 99–105.
- [22] C.P. Chen, C.-Y. Tsao, Acta Mater. 45 (1997) 1955–1968.